Energy transfer in close-packed PbS nanocrystal films

V. Rinnerbauer, H.-J. Egelhaaf, and K. Hingerl
Christian Doppler Laboratory of Surface Optics, Institute of Semiconductor and Solid State Physics, University Linz, Altenbergerstrasse 69, A-4040 Linz, Austria

P. Zimmer, S. Werner, T. Warming, and A. Hoffmann
Institute of Solid State Physics, Technical University Berlin, Hardenbergstrasse 36, D-10623 Berlin, Germany

M. Kovalenko, W. Heiss, G. Hesser, and F. Schaffler
Institute of Semiconductor and Solid State Physics, University Linz, Altenbergerstrasse 69, A-4040 Linz, Austria
(Received 23 August 2007; revised manuscript received 12 December 2007; published 26 February 2008)

We study the emission properties of close-packed films of PbS nanocrystals that show emission in the infrared. In time resolved photoluminescence measurements, we observe a fast decay time of ~400 ps and a slow component between 20 and 80 ns, depending on the temperature, which are attributed to decay from core and surface states, respectively. Photoluminescence excitation and temperature-dependent photoluminescence measurements show that these states are coupled by thermal activation and energy transfer. These transfer processes efficiently replenish the core states with charge carriers from the surface states, increasing the photoluminescence yield.

DOI: 10.1103/PhysRevB.77.085322 PACS number(s): 78.67.Bf, 78.55.−m

I. INTRODUCTION

Nanocrystals (NCs) are nanometer sized semiconductor crystallites, often also called quantum dots, which exhibit unique properties compared to the respective bulk semiconductor material. When the size of the crystallites is reduced below the exciton Bohr radius, electronic and optical properties of the NCs become size dependent as the electronic excitations are spatially confined to the volume of the NC. Due to quantum confinement in the NC, the bulk band structure is quantized, and electronic transitions become discrete and shift to higher energies with decreasing NC diameter. The possibility to tune the emission energy together with the development of reliable colloidal synthesis methods[1] has spurred research on NCs and has led to the development of interesting applications in optoelectronics[2–4] and biology.[5] Nanocrystals of lead salts are a showcase example for a strong confinement of charge carriers due to their large exciton Bohr radius (a_B=18 nm for PbS). Therefore, large quantization energies are expected,[6] which permit us to shift the transition energies of these small band gap materials across a wide range of the infrared spectrum, turning lead-salt NCs into an attractive material both for applications as well as fundamental studies in the strong confinement regime.

In close-packed films of NCs as opposed to NCs in solution, coupling between the NCs can occur. This coupling has been a topic of numerous studies[7,8] and has been explained by Förster resonant energy transfer,[9] a radiationless dipole-dipole interaction. With the help of this coupling, excitation energy can efficiently be transferred between different NCs, an effect that has been used in applications such as biosensors[10] and light-emitting devices.[11] Recently, a close-packed layered NC film has been demonstrated not only to efficiently transfer excitation energy to a desired emission energy, but also to increase the emission intensity by recycling of otherwise trapped excitons.[12,13] In this optimized structure with a gradient of NC sizes across the layered film, the photoluminescence yield could be increased by a factor of more than 4.

In our work, we study close-packed films of PbS NCs, which are nominally monodisperse and are deposited from colloidal solution without any size-selective or spatial arrangement. Nevertheless, we can observe coupling of the NCs and an increase of the photoluminescence intensity by a factor of 6 through the release of charge carriers trapped in surface states to the emitting states. The efficiency of this process only depends on the deposition parameters (spin cast or drop cast) and the resulting average distance of the NCs.

In particular, we investigate the emission properties of close-packed films of PbS NCs with diameters of about 5 nm, emitting in the near infrared with photoluminescence (PL) energies around 0.9 eV at room temperature. We employ PL measurements under continuous excitation from liquid helium to room temperature as well as time resolved photoluminescence (TRPL) measurements and photoluminescence excitation (PLE) experiments, and establish a model for the transition states and processes involved in luminescence.

II. EXPERIMENTS

We use ligand-capped PbS NCs from a colloidal solution, which exhibit PL at wavelengths of about 1430 nm in solution at room temperature. The NCs are deposited from toluene solution on silicon on insulator (SOI) substrates either by drop casting or by spin casting, resulting in layers of different thicknesses and densities. Spin casting results in a smooth and homogeneous film, whereas during drop casting, the drop forms areas of varying thickness with cracks and voids as it dries up. In addition, NCs were dispersed in polymethyl methacrylate (PMMA) as a matrix and were then spin cast on the substrates. By spectroscopic ellipsometry (SE), we determined the NC layer thickness of these films as well

TABLE I. NC layer thickness, volume concentration c_{vol} determined from SE, calculated average distance in units of NC diameter and nanometer, and interparticle separation between NCs.

Preparation method	Thickness (nm)	c_{vol} (%)	Distance (d_{nc})	Distance (nm)	Separation (nm)
Drop cast	729	26.9	1.40	7.0	2.0
Spin cast	45	27.8	1.39	6.9	1.9
PMMA	154	0.17[a]	7.63	38.2	33.2

[a]From mass concentration in dispersion.

as the density of the NCs deposited from toluene solution, modeled with an effective medium approximation[14] as a compound layer of PbS NCs in void. For the NCs dispersed in PMMA, we calculate the volume concentration of the NCs from their mass concentration used in the preparation of the dispersion. From the volume concentration, we can determine the average distance between the NCs (see Table I). For the NCs deposited from solution, the SE measurements give a volume concentration of about 27%. This volume concentration leads to an average distance of 1.4 times the diameter of the NCs ($d_{nc} \sim 5$ nm), which means that the interparticle separation is only 2 nm. This is not more than twice the thickness of the ligand shell, constituting a close-packed arrangement. Scanning electron microscope (SEM) pictures (Fig. 1) were taken to clarify the morphology of the films. They show the formation of cracks on the surface of the spin cast samples, which are not penetrating the spin cast layer, which is homogeneously dense across the thickness of the layer as can be seen in the side view of a cut formed by focused ion beam [Fig. 1(c)]. In the drop cast layer, substantial holes and voids can be seen between clusters of NCs in the side view of the layer [Fig. 1(d)].

Although the ellipsometry measurement gives a slightly lower average NC concentration for the drop cast sample, we have to take into account the holes and voids formed while drying, which entails that the actual distance between the nanoparticles in the clusters is lower in the drop cast sample. In contrast to the dense NC films formed from solution, the volume concentration of the NC dispersion in PMMA is only 0.17%, which leads to an average distance of 7.6 times the diameter of the NCs, i.e., about 33 nm interparticle separation on average. Although the dispersion is homogeneous on a macroscopic scale, the distance between NCs may vary due to aggregation.

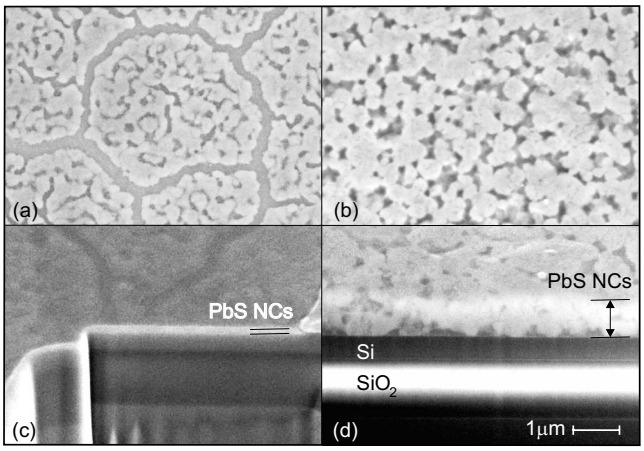

FIG. 1. SEM picture of PbS NCs deposited by spin casting (left) and drop casting (right) on SOI substrates from top view [(a) and (b)] and side view [(c) and (d)]. Cracks are visible on the surface of the spin cast samples (a) but not on the side view showing a homogeneously dense layer (c), whereas the side view of the drop cast samples (d) reveals cluster formation and voids.

We measured PL under continuous excitation (cw) in a helium flow cryostat for temperatures starting from 20 K to room temperature under excitation by a frequency doubled Nd:YVO laser with emission wavelength of 532 nm and excitation powers of 10–100 mW. PL was detected by a Peltier-cooled InGaAs detector array.

TRPL was measured at 2 K and at room temperature. For excitation, a dye laser with a pulse width of <3 ps was used at a wavelength of 586 nm. The decay of the PL signal was observed by time correlated single photon counting using a microchannel plate photomultiplier tube (type R3809U-69M by Hamamatsu) as detector. The observed signal was deconvoluted with the detector response function to extract the PL decay.

For the same sample set examined in TRPL, PLE experiments were performed at 7 K and at room temperature. First, PL spectra of the NC samples were taken, and then PL was detected selectively for different detection energies near the PL peak energy while varying the excitation from the detection energy up to 1.6 eV using a halogen lamp for excitation.

III. RESULTS

A. Photoluminescence

We investigate the temperature dependence of PL under continuous excitation for PbS NC spin cast and drop cast from solution from 20 K to room temperature. As one can see from the respective PL spectra (Fig. 2), the samples prepared by these different methods show fundamentally different behaviors. First of all, at room temperature, we observe that the emission of the drop cast NCs is redshifted with respect to the spin cast ones by more than 70 meV. For both, the PL peak shifts to the red with decreasing temperature. The PL energy decreases approximately linearly with decreasing temperature. Above 100 K, the decrease amounts to 0.31 and 0.39 meV/K for the drop cast and the spin cast NCs, respectively, with a decreasing temperature coefficient below 100 K [see Fig. 3(a)]. The band gaps of lead salts have a positive temperature coefficient, which is 0.52 meV/K for bulk PbS in the temperature range of

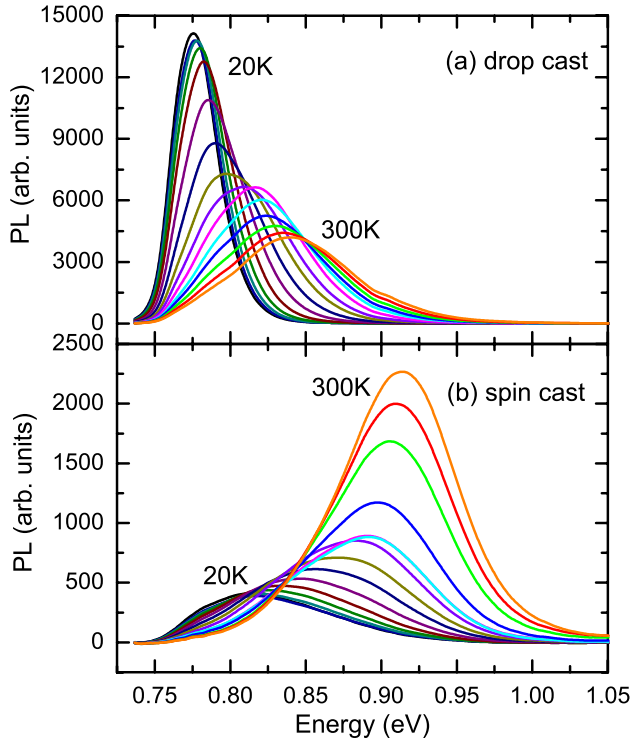

FIG. 2. (Color online) PL spectra of PbS NCs (a) drop cast and (b) spin cast on silicon substrates taken at different temperatures.

100–400 K.[15] For NCs, this temperature coefficient decreases with decreasing radius[16] as it goes toward zero for a zero dimensional energy state. Regarding the PL intensity, we see a profound difference in the temperature-dependent PL behavior for the spin cast and the drop cast samples. Whereas the integrated PL intensity increases with increasing temperature by a factor of 5 for the spin cast NCs, it decreases by about 40% for the drop cast NCs [see Fig. 3(b)]. The linewidth [full width at half maximum (FWHM)] of the PL spectrum is almost constant for the spin cast NCs, whereas it decreases with decreasing temperature for the drop cast ones [see Fig. 3(c)].

The temperature dependence of the PL is very sensitive to the parameters of the preparation method and the resulting distance between the NCs. As a consequence, the two opposite temperature dependencies of PL intensity have been observed to a varying degree in spin cast and drop cast samples depending on the preparation parameters. For NCs dispersed in PMMA, both trends were observed in different samples. Despite the large average distance between the particles in PMMA, the NCs tend to aggregate in the polymer matrix; therefore, the real distance may vary from sample to sample.

The observed behavior indicates that different processes are involved in PL, which supply charge carriers to the emitting state and contribute to the PL intensity. To examine the mechanisms involved in PL further, we performed time resolved PL measurements and PL excitation measurements at liquid helium and room temperature.

B. Time resolved photoluminescence

Time resolved photoluminescence measurements were performed at 2 K and at room temperature on close-packed

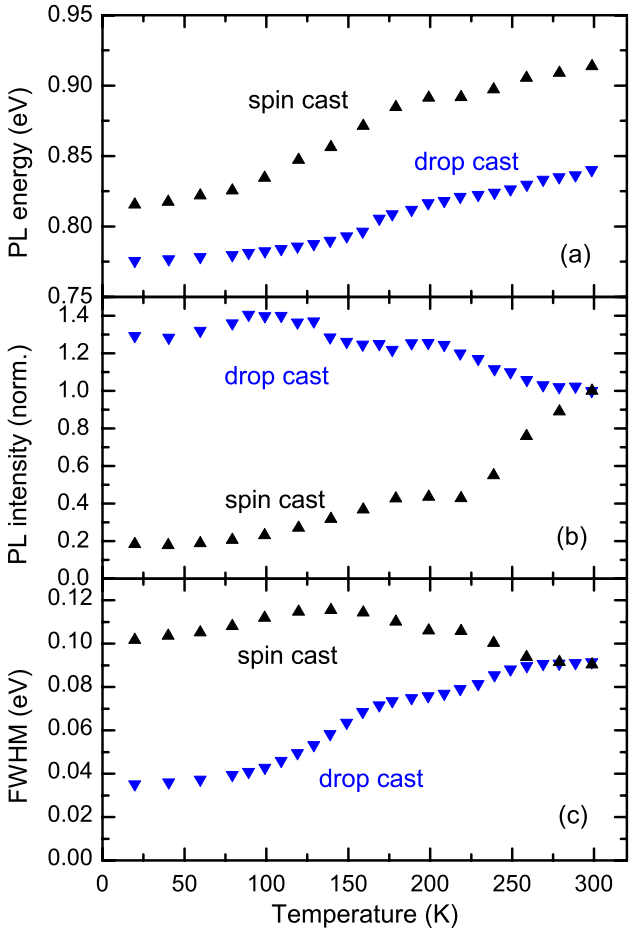

FIG. 3. (Color online) (a) PL energy, (b) normalized intensity, and (c) FWHM of PbS NCs spin cast and drop cast on silicon substrates.

NC films prepared by drop casting and spin casting PbS NCs from solution (Fig. 4). We observe photoluminescence decay with two time constants, a fast component τ_1 (<1 ns) and a slow component τ_2 (approximately tens of nanoseconds), whose decay times depend on the temperature and the detected PL wavelength (see Table II). The presence of two distinct time constants indicates that two types of excited states are present in our NC films.

The decay time of the fast component τ_1 shows different temperature behaviors for drop cast and spin cast NCs. It decreases with increasing temperature for the spin cast NCs by a factor of 3, from 0.6 to 0.2 ns, whereas the decrease for the drop cast ones is only $\sim$20%. For both preparation methods, the decay times are almost constant across the PL spectrum.

The decay time of the slow component τ_2 decreases with increasing temperature for drop cast NCs by a factor of more than 3, and for the spin cast ones by a factor of 2. Regarding the dependence on wavelength, the decay times of the slow decay increase with increasing wavelength, i.e., with increasing NC size, and exceed the time window of the measurement (70 ns) for higher wavelengths.

We also observe the relative amplitudes of the fast to the slow component A_1/A_2 with temperature. For the spin cast

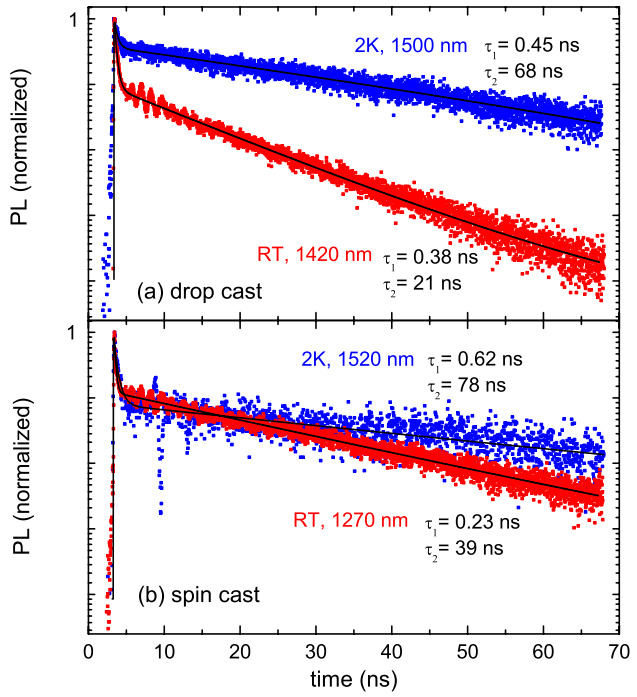

FIG. 4. (Color online) PL transients of PbS NCs (a) drop cast and (b) spin cast on silicon substrate measured at 2 K (blue) and room temperature (red).

NCs, the amplitude of the fast decay is higher than that of the slow decay both at room and at low temperature, with a ratio of 1.3 at room and 1.9 at low temperature. In the case of the drop cast NCs, the amplitude of the fast decay relative to the slow decay is 1.8 at room temperature and decreases to 0.4 at 2 K.

PL decay times reported so far on PbS NCs in solution were on the order of hundreds of nanoseconds to microseconds.[17–20] The long decay times were attributed to trapping and detrapping processes in deep trap states. In reports of PbSe NCs long decay times (approximately hundreds of nanoseconds) were observed and attributed to dielectric screening owing to the high dielectric constant of PbSe. As pointed out by Allan and Delerue,[21] the radiative lifetime depends on the dielectric surrounding of the NCs. This can be taken into account by a local field factor F

TABLE II. Decay times at about peak PL wavelength from TPRL for PbS NCs drop cast and spin cast on silicon substrates at 2 K and at room temperature.

T (K)	λ (nm)	τ_1 (ns)	τ_2 (ns)	A_1/A_2
		Drop cast		
2 K	1500	0.45	67.9	0.43
300 K	1420	0.38	20.8	1.77
		Spin cast		
2 K	1520	0.62	78.0	1.88
300 K	1270	0.23	38.7	1.34

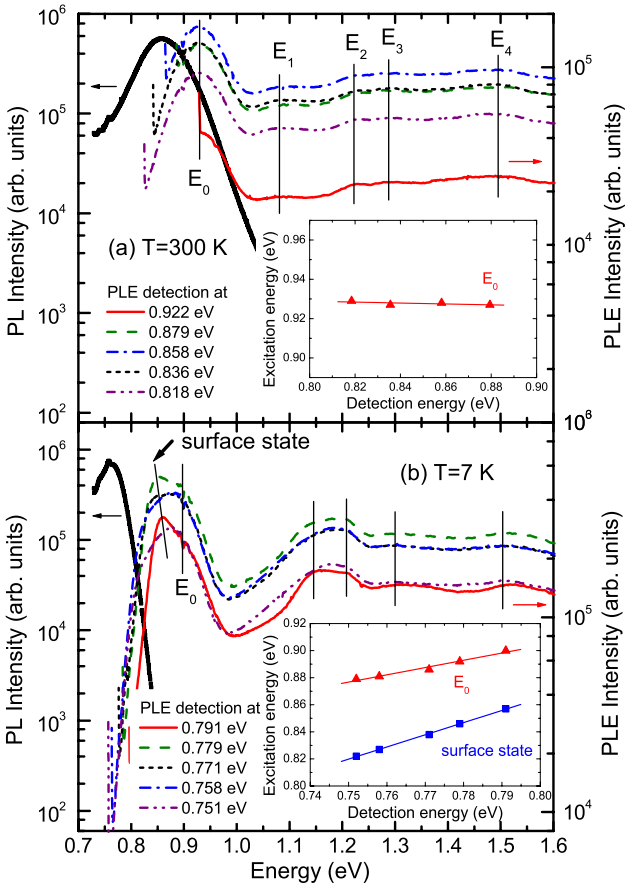

FIG. 5. (Color online) PL and PLE of PbS NCs drop cast on silicon substrate at room temperature (top) and at 7 K (bottom).

$\approx 3\epsilon_{out}/(\epsilon_{in}+2\epsilon_{out})$ in the decay rate, where ϵ_{out} and ϵ_{in} are the dielectric constants outside and inside the NC, respectively. The corresponding decay time decreases with the square of the field factor, $\tau \propto 1/F^2$ For PbSe NCs, the radiative lifetime was calculated[21] to be about 10^{-6} s in solution with $\epsilon_{out}=2.1$ and 10^{-8} s with $\epsilon_{out}=\epsilon_{in}=23$. For a close-packed film as in our case, the radiative lifetime would therefore be 2 orders of magnitude smaller than for NCs in solution, as were investigated in previous reports,[17–20] even without taking into account any effect of coupling between the NCs in close-packed films.

C. Photoluminescence excitation

PLE spectra were taken at 7 K and at room temperature for the same set of samples as in TRPL, drop cast (Fig. 5) and spin cast (Fig. 6) from solution. In these spectra, we observe up to five excitation peaks in the energy range of 0.7–1.6 eV, with energies depending on the preparation method and the temperature. The spectra were taken at different detection energies chosen across the PL spectrum. These detection energies correspond to emission from NCs of different sizes. For uncoupled NCs, one would expect the excitation peaks in the PLE spectra to shift with the detection energy. At room temperature, there is no change in the PLE spectrum for different detection energies, i.e., NC sizes,

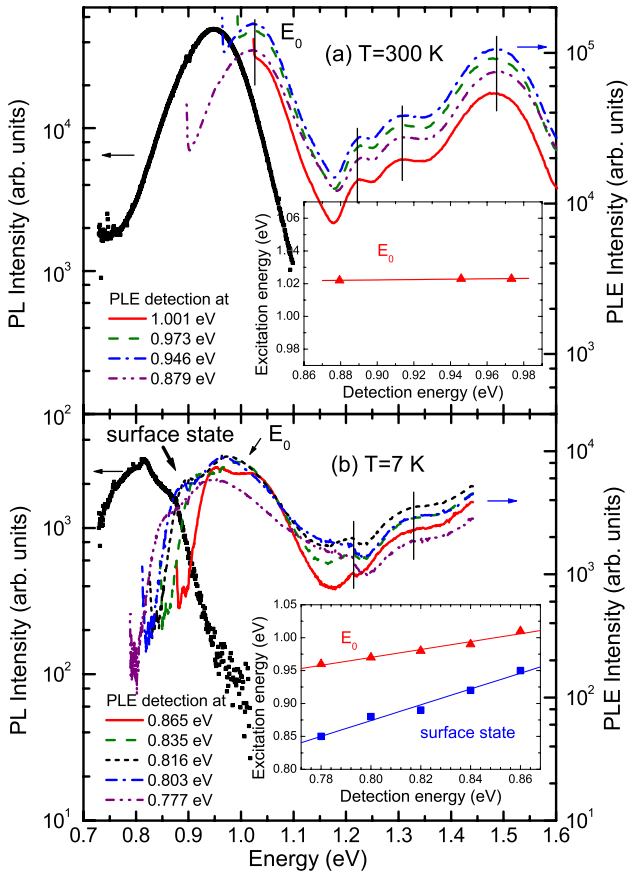

FIG. 6. (Color online) PL and PLE of PbS NCs spin cast on silicon substrate at room temperature (top) and at 7 K (bottom).

which indicates that the NCs are coupled. The energies of the peaks in the PLE spectra were determined from the derivative and correspond very well to energy levels as calculated after the experimentally determined formula of Cademartiri *et al.*[22] for NCs with a radius of about 2.5 nm (see Table III for the drop cast NCs at room temperature). For the drop cast NCs, the first transition energy is 0.93 eV at room temperature, whereas for the spin cast NCs, it is 1.02 eV. Also, the higher transition energies are slightly shifted from the values of the drop cast NCs. First principles calculations predict similar values[6,23] for the lowest exciton energies of PbS NCs.

In the low temperature PLE spectra of both drop cast and spin cast NCs, another peak is observed on the low energy side of the first excited state, marked by an arrow in Figs. 5(b) and 6(b). This peak becomes more dominant for higher detection energies, i.e., smaller NC size. Its position shifts to higher energies with increasing detection energy [see insets of Figs. 5(b) and 6(b), "surface state"], so that the energy difference to the PL detection energy is approximately constant at about 67 meV for the drop cast and 78 meV for the spin cast NCs, indicating a constant binding energy between absorbing and emitting states. In contrast to this, the shift of the E_0 transition in the PLE spectra with detection energy is much less pronounced with a slope of 0.54 and 0.6 for drop cast and spin cast NCs, respectively [see insets of Fig. 5(b) and 6(b)]. Obviously, there is still some coupling between the absorbing NCs for this transition, even though not as strong as at room temperature.

IV. DISCUSSION

The diametrical experimental results observed in temperature-dependent PL measurements (Fig. 2) can be explained if we consider surface states as well as energy transfer between the NCs. Interparticle energy transfer not only couples NCs of different sizes, changing the emission spectrum, but also efficiently reactivates the excitation energy trapped in the surface states and thus replenishes charge carriers to the emitting states. With increasing temperature, thermal activation of the charge carriers in the surface states plays another important role. The interplay of both processes and their contribution to the PL yield explains the observed effects, namely, (a) the suppression of an energy shift of the PLE spectra with detection energy, (b) the temperature dependencies of the two components in the PL decay, and (c) the increase or decrease of PL intensity and linewidth with temperature depending on sample preparation. We establish the following model for the transition processes in the NCs, which explains our experimental results as discussed below.

A. Model

We model the two decay times observed in our TRPL experiments with the existence of two different energy states: a "core" state in the following labeled 1 and a "surface" state labeled 2. Taking into account the size distribution of the NCs, we establish a general model for the decay from those two states, as pictured in Fig. 7. The decay of the charge carrier populations N_1 of the core state and N_2 of the surface state occurs, on one hand, via recombination to the ground state with the respective transfer rates k_1 and k_2, whereby we assume that $k_1 \gg k_2$ in our system. In the most general case, the recombination rates of the core and surface states k_1 and k_2 both consist of a radiative term k^{PL}, a nonradiative term k^{NR}, and a term corresponding to the energy transfer rate k^{ET} between the same states of NCs of different sizes, from core to core or from surface to surface.

TABLE III. Transition energies E_i calculated after Ref. 22 for NC radius r=2.5 nm and determined from PLE measurements at room temperature for drop cast PbS NCs.

	E_0 (eV)	E_1 (eV)	E_2 (eV)	E_3 (eV)	E_4 (eV)
Calculated	0.91	1.10	1.25	1.27	1.50
Measured	0.93	1.09	1.21	1.29	1.48

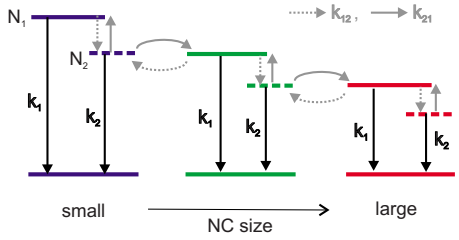

FIG. 7. (Color online) Decay model for NC ensembles of various sizes considering core and surface states and coupling between them.

$$k_1 = k_1^{PL} + k_1^{NR} + k_1^{ET}, \quad k_2 = k_2^{PL} + k_2^{NR} + k_2^{ET}. \tag{1}$$

In addition to recombination to the ground state, there is a transfer between the two excited states, from core to surface state with rate k_{12} and from surface to core state with rate k_{21}. This transfer can take place either by thermal activation with the help of phonons between the states of one NC (intra-NC) or by energy transfer between the states of adjacent NCs of different sizes (inter-NC), which is possible without energy uptake.

The resulting rate equations are

$$\frac{dN_1}{dt} = -k_1 N_1 + k_{21} N_2 - k_{12} N_1,$$

$$\frac{dN_2}{dt} = -k_2 N_2 - k_{21} N_2 + k_{12} N_1. \tag{2}$$

Since in our system the decay rate k_1 is 2 orders of magnitude higher for the core state than k_2 for the surface state, the population N_1 of the core state is emptied fast, and for $t \gtrsim 0.5$ ns the last term in Eq. (2) is negligible compared to the second term, resulting in a net flow of charge carriers from surface to core states. For this reason, the terms with k_{12} are not considered in the following discussion.

With N_{surf} and N_{core} being the initial population of surface and core states after excitation, the rate equations yield

$$N_1(t) = \left(N_{core} - \frac{k_{21}}{k_1 - (k_2 + k_{21})} N_{surf} \right) e^{-k_1 t} + \frac{k_{21}}{k_1 - (k_2 + k_{21})} N_{surf} e^{-(k_2 + k_{21})t}, \tag{3}$$

$$N_2(t) = N_{surf} e^{-(k_2 + k_{21})t} \tag{4}$$

for the decay of the population of core and surface states with time. In Eq. (3), the first exponential term refers to the decay of the population of the core state to the ground state, whereas the second exponential function models the replenishing by the transfer of charge carriers from the surface state. As a consequence, we obtain two contributions to time-dependent PL with the two decay times k_1 and $k_2' = k_2 + k_{21}$ with different amplitudes A_1 and A_2,

$$\mathrm{PL}(t) = A_1 e^{-k_1 t} + A_2 e^{-k_2' t}, \tag{5}$$

where

$$A_1 = k_1^{PL} N_{core} - k_1^{PL} \frac{k_{21}}{k_1 - k_2'} N_{surf},$$

$$A_2 = k_2^{PL} N_{surf} + k_1^{PL} \frac{k_{21}}{k_1 - k_2'} N_{surf}. \tag{6}$$

The second term in Eq. (6) corresponds to the transfer from surface to core states, which decreases the ratio of the amplitudes A_1/A_2. The first term of the amplitude A_2 is the contribution of recombination from the surface state to PL, which is small due to the small quantum yield of the surface state. If there is an efficient transfer from surface to core states by thermal activation or by inter-NC energy transfer, the transferred charge carriers can recombine from the core states with the much higher rate k_1 and higher quantum yield. By this way, the overall PL yield is increased by coupling of the surface to the core states.

As discussed above, the transfer from surface to core states results from two processes: on one hand, thermal activation of charge carriers from the surface state in the same NC (intra-NC) by annihilation of phonons and, on the other hand, energy transfer from surface states of smaller NCs to resonant core states of larger NCs (inter-NC) without energy increase. In short, this has the following consequences: Thermal activation is present in both drop cast and spin cast samples, its efficiency and the resulting contribution to PL increasing with $\propto e^{-E_a/k_B T}$ as an activation energy $E_a \approx 70$ meV has to be overcome from surface to core states. This effect is observed as an increase of PL intensity with increasing temperature in the cw PL measurements of the spin cast NCs. Inter-NC energy transfer, on the other hand, depends on the distance between the NCs and is only efficient in the (denser) drop cast NC films. The size distribution leads to an energy spread of the core states, which is of the same order of magnitude as the thermal activation energy; therefore, this inter-NC energy transfer is only observed at low temperatures and diminishes with increasing temperature in favor of thermal activation. The contribution of energy transfer to the PL yield can therefore be observed for the drop cast NCs at low temperatures, which counterbalances or even exceeds the contribution of thermal activation.

B. Core and surface states

We attribute the fast decay time observed in the TRPL experiments (Fig. 4) to the core states with decay rate k_1 and the slow component to the surface states with decay rate k_2'. As discussed in Sec. III C, we observe in the PLE spectra an additional peak at the low energy side of the first excited state at low temperatures (Figs. 5 and 6). This peak is attributed to the resonant excitation of the core state and the subsequent (partial) decay to the surface state of the same NC, where charge carriers recombine radiatively. At higher temperatures, this peak vanishes due to thermal transfer to core states, and PL from the surface state is not observed due to the long lifetime of these states. The surface PL peak at low temperature is more prominent for smaller NCs, i.e., higher detection energy, because of their higher surface-to-volume ratio. The energy of this surface state shifts with the detec-

tion energy, i.e., with NC size. The energy difference between the absorbing core state and the emitting surface state is constant at about 67–78 meV for drop cast and spin cast samples, respectively. Even though charge carriers in the surface state are localized, they still feel the effect of quantum confinement due to the small NC size (r=2.5 nm), which is much smaller than the exciton Bohr radius (a_B=18 nm for PbS). Therefore, the energy of this surface state shifts with NC size just like the band gap resulting in a constant binding energy.

It has been shown recently for CdSe that surface states can also give a significant contribution to luminescence.[24] Fernée *et al.* [20] found that in small PbS NCs (~1–2 nm), luminescence stems from a hybrid state where holes are localized in a surface state, leading to a size-dependent Stokes shift. In other studies of small PbS NCs[18,19] with emission energies around 2 eV, multiple emission peaks attributed to emission from deep traps were reported, with accordingly large Stokes shifts of up to 0.5 eV. The measured PL decay times for these transitions were on the order of microseconds, attributed to trapping and detrapping processes leading to delayed luminescence. In our case, Stokes shifts are much smaller, ranging from 70 meV at room temperature to 170 meV at 7 K (see Figs. 5 and 6). The small Stokes shift as well as the short lifetimes indicate band edge emission rather than emission from surface states. This was also found in PbSe NCs with near-infrared emission and small Stokes shifts.[25,26]

For surface states with lower energy to be populated from core states, an energy barrier has been found in previous studies of CdTe NCs.[12,13] This barrier can only be overcome at elevated temperatures and with the help of coupling to phonons. Charge transfer by thermal activation from exciton states to deep trap states was already observed previously[18,19] for small PbS NCs emitting in the visible, increasing the PL intensity of lower energy trap states with increasing temperature and decreasing emission from the higher energy exciton state. In that case, however, the lifetimes of the observed states were comparable and on the order of microseconds. In our case, the lifetime of the emitting core state is at least 2 orders of magnitude smaller than that of the surface state. For this reason, the net transfer occurs in the other direction from surface to core states, replenishing the core states, which are depleted fast, from slowly decaying surface states.

C. Coupling between nanocrystals

The evidence of the transfer of excitation energy across the size distribution of NCs can be seen in the PLE spectra (see Figs. 5 and 6) where clearly the absorbing states are coupled since there is no difference in the absorbing spectra for different emission energies at RT and there is only a small shift less than the difference in PL energy at low temperatures. Due to the size distribution of the NCs and its inhomogeneous contribution to the PL spectrum, the PLE spectrum should shift with PL detection energy, i.e., with the size of the emitting NCs. Recently, the linewidth of 3 nm PbS NCs was determined by single NC spectroscopy,[27] and it was shown that the homogeneous (i.e., intrinsic) linewidth makes up for a large part (one-fourth) of the spectral linewidth of the NC ensemble with a size distribution of σ =15%. Fernée *et al.*[28] determined the homogeneous and inhomogeneous contributions to the PL linewidth of 2.5 nm PbS NCs with a size distribution of σ=12% and found a large homogeneous component (FWHM of 170 meV) compared to a smaller inhomogeneous contribution (FWHM of 110 meV) arising from the size distribution. This broad homogeneous linewidth, together with a large temperature-dependent component of the linewidth, is attributed to an enhanced coupling with acoustic phonons. Even though they show that the spectral shape of their NCs is mainly determined by the homogeneous linewidth, the PLE spectra they measured for NCs in solution show a clear energy shift with detected emission wavelength corresponding to absorption in NCs of different sizes.[20] In contrast to this, this energy shift of the PLE spectra is suppressed in our measurements of close-packed NC layers on substrates. This indicates that in our case the excited states of the NCs are coupled by energy transfer across the size distribution. This coupling is not observed in Refs. 20 and 28 because in solution the NCs are well separated.

Although the coupling of the NCs across the size distribution is evident from the experimental observations, the nature of this coupling is not clear from our experiments. Coupling of NCs of different sizes has been observed before in close-packed films of CdSe,[7,8,29] CdTe,[30,31] InP,[32] and PbS (Ref. 33), both in mixtures of NCs of different sizes and in films of nominally monodisperse NCs due to their inhomogeneous size distribution. In films of NCs with mixed sizes, this coupling has been demonstrated to efficiently suppress the PL emission of the smaller NCs and to enhance the PL emission of the larger NCs with smaller emission energy. For nominally monodisperse NCs, the coupling was observed by a redshift of the PL spectra and by a narrowing of the emission line shape corresponding to the unidirectional excitation energy flow from smaller to larger NCs. In addition, a decrease of the PL decay time compared to NCs in solution has been observed as well as the decrease of decay time with decreasing PL wavelength. Kagan *et al.*[7] first attributed the observed effects to a long range resonant transfer, which, according to their findings, describes the observed decay times of the coupled NCs better than exciton diffusion.

Förster transfer (FRET) is a nonradiative dipole-dipole coupling mechanism,[9,34] which depends on the overlap of the emission spectrum of the donor and the absorption spectrum of the acceptor, the quantum yield of the donor, as well as very sensitively on the distance between donor and acceptor (r^{-6}). For efficient FRET, the emission and absorption spectra of the involved NCs have to match spectrally, and matching donors and acceptors have to be found in a close neighborhood. Förster radii on the order of 5–8 nm for close-packed PbS NCs with 2–2.5 nm diameter[33] have been found, and, equally, for CdSe and InP NCs calculated Förster radii are on the order of several nanometers.[7,32] In optimized layered films of CdTe NCs, Förster transfer times as fast as 50 ps could be observed.[31] Since in our case of nominally monodisperse NCs donor and acceptor NCs are the same species, the linewidth of the PL spectrum is about 100 meV, and the energy shift between absorption and emission is on

the same order of magnitude (see Figs. 5 and 6), we would have expected the efficiency of FRET to be lower. In the PLE spectra, we observe the coupling between the core states of NCs of different sizes, which are responsible for the main contribution to cw PL. In our decay rate model, this process gives a contribution to the decay rate k_1 of the core states. In the drop cast NC films, we observe, in addition, the impact of FRET from surface states, which leads to an increase of intensity and decrease of linewidth at low temperatures, as discussed in the next section. In addition, the PL spectrum is observed at lower energy for the drop cast NCs, which can be ascribed to a redshift of the spectrum because of energy transfer from smaller to larger NCs.

Although FRET explains the observed effects very well, other forms of coupling such as electronic transfer of single charge carriers or exciton diffusion cannot be excluded. In single NC spectroscopy,[27] blinking of the NCs was observed, which is attributed to tunneling of charge carriers out of the NC core. The good photoconductivity of PbS NCs has led to the development of solution-cast PbS NC photodetectors with outstanding sensitivity.[4] Therefore, transfer of excitation energy by charge transfer between NCs is conceivable as well and would lead to similar effects as observed in our experiments.

D. Energy transfer from the surface states

Transfer of excitation energy not only takes place between the core states of NCs of different sizes, but also from surface states to core states of larger NCs. In fluorescence spectroscopy, FRET is known to transfer energy from trap states to radiative states, thus efficiently reactivating charge carriers trapped in surface states and increasing the PL yield. Franzl and co-workers[12,13] realized an optimized NC layer structure, which increased the PL yield by a factor of more than 4 through recycling of excitons from surface to emitting states along a size gradient of the NCs.

We observe the impact of this process both in the transient PL experiments as well as in the cw PL measurements. In our model, the transfer process is taken into account by a contribution to k_{21}, which describes the transfer of charge carriers from the surface to the core states. This transfer rate can be observed as a component of the decay rate of the surface state k_2' in addition to the radiative and nonradiative decay processes of the surface state, and therefore as a decrease of the slow component τ_2 of the decay time in our TRPL experiments. As discussed in Sec. IV A, the other contribution of this coupling of the states k_{21} is by thermal activation of charge carriers from the surface states to the core states in the same NC (intra-NC), which increases with temperature as $\propto e^{-E_a/k_BT}$. In our TRPL experiments, we see that the decay time of the slow surface component τ_2 decreases with temperature by a factor of up to 3 (Table II), which reflects the increasing contribution of the thermal intra-NC transfer process to the population of the surface states. Of course, the other decay processes, radiative and nonradiative, also depend on the temperature, and the respective contributions to the temperature dependence of the decay time cannot be distinguished.

In contrast to the thermal process, the reactivation of charge carriers from surface to core states by energy transfer between NCs (inter-NC) does not depend explicitly on the temperature. Since this process is in competition with other decay processes, its contribution is higher at low temperatures when thermal activation vanishes, whereas at higher temperatures energy transfer from surface to core states diminishes in favor of thermal activation. In TRPL, we observe that the magnitude of the amplitude of the fast decay relative to the slow decay A_1/A_2 is decreased for the drop cast NCs from $\sim$1.8 at room temperature to $\sim$0.4 at low temperature (see Table II). The reason for the decrease is the increased inter-NC energy transfer from surface to core states at low temperature in the drop cast NCs, which increases the amplitude A_2 of the PL stemming from charge carriers replenished from the surface states [see Eq. (6)]. In contrast to the drop cast NCs, the fast amplitude is always higher than the slow amplitude for the spin cast NCs regardless of the temperature. In this case, the ratio of the amplitude of the fast component relative to the slow component decreases with temperature, which shows the contribution of charge carriers reactivated by thermal transfer from the surface to the core state.

The transfer process from surface to core state intra-NC as well as inter-NC is also observed in cw PL. The main contribution in PL stems from the radiative decay of the core states with a short lifetime, whereas the surface states decay on a much longer time scale. Via thermal activation as well as energy transfer, the core states are replenished by charge carriers from the surface states and contribute to the PL intensity by radiative recombination from the core states. The supplies of charge carriers from the surface to the core states by energy transfer (inter-NC), on one hand, and thermal activation (intra-NC), on the other hand, both contribute to the cw PL yield with different dependencies on the temperature, which explains the different temperature-dependent behavior of cw PL for the drop cast and the spin cast NCs. The contribution of thermal activation to the PL yield increases with increasing temperature, as can be observed for the spin cast NCs [Fig. 3(b)]. The PL intensity of spin cast NCs was fitted with a Boltzmann temperature dependence $\propto e^{-E_a/k_BT}$. This gives an activation energy from the surface to the core state of E_a=66 meV, which is in good agreement with the binding energy found in the PLE experiments of 78 meV for spin cast and 67 meV for drop cast NCs.

In contrast to thermal activation, the contribution of energy transfer as a competing process diminishes with increasing temperature in favor of thermal activation, so it is strongest at low temperatures. Since energy transfer is always directed from smaller to larger NCs, it also decreases the PL linewidth. This influence of the energy transfer can be observed for drop cast NCs as an increase of PL intensity at low temperatures and the decrease of FWHM [Fig. 3(b) and 3(c)]. It increases the PL intensity at low temperatures by more than a factor of 6 when compared to the spin cast NCs. For comparison, we normalize the PL intensity to the value at room temperature, where mainly thermal activation from the surface states (intra-NC) occurs for samples of both preparation methods. The FWHM is decreased by more than a factor of more than 2 from room temperature to 20 K. The

reason why the energy transfer from surface to core states cannot be observed in the spin cast NCs lies in the high sensitivity of the efficiency of the energy transfer on the distance between the NCs. This distance between the NCs depends highly on the parameters of the preparation of the NC films. In both methods, spin casting and drop casting of NCs from solution, close-packed films of NCs are formed. In the drop cast NC films, however, the particles are more densely packed between the voids formed while drying from solution, whereas the distance between the NCs is higher when deposited homogeneously by spin casting. This is why the (inter-NC) energy transfer from surface to core states only plays a significant role in the drop cast NCs.

V. CONCLUSION

We investigate the optical properties of close-packed films of nominally monodisperse NCs. Depending on the sample preparation and the resulting NC density, we observe an increase of PL intensity with temperature for spin cast (less dense) NCs or a decrease for drop cast (more dense) NCs. PLE measurements reveal an efficient coupling of the emitting states across the size distribution of the NCs. We measure decay times of PbS NCs at liquid helium and at room temperature and observed a fast (~400 ps) and a slow (approximately tens of nanoseconds) component of the decay time. We model these with charge carrier recombination from core and surface states, respectively. These states are coupled by thermal activation and by energy transfer, both of which transfer charge carriers from the surface to the core state. The subsequent supply of charge carriers to the core states by transfer from the surface states leads to an increase of PL intensity under continuous excitation.

ACKNOWLEDGMENTS

This work was supported by the EU STREP Project N2T2 (IST-NMP2-2004-017481). Financial support from the FWF (Project Start Y179 and SFB: IRON) is acknowledged.

[1] C. B. Murray, S. Sun, W. Gaschler, H. Doyle, T. A. Betley, and C. R. Kagan, IBM J. Res. Dev. **45**, 47 (2001).
[2] V. L. Colvin, M. C. Schlamp, and A. P. Alivisatos, Nature (London) **370**, 354 (1994).
[3] S. Coe, W. K. Woo, M. Bawendi, and V. Bulovic, Nature (London) **420**, 800 (2002).
[4] G. Konstantatos, I. Howard, A. Fischer, S. Hoogland, J. Clifford, E. Klem, L. Levina, and E. H. Sargent, Nature (London) **442**, 180 (2006).
[5] M. Bruchez, M. Moronne, P. Gin, S. Weiss, and A. P. Alivisatos, Science **281**, 2013 (1998).
[6] I. Kang and F. W. Wise, J. Opt. Soc. Am. B **14**, 1632 (1997).
[7] C. R. Kagan, C. B. Murray, and M. G. Bawendi, Phys. Rev. B **54**, 8633 (1996).
[8] S. A. Crooker, J. A. Hollingsworth, S. Tretiak, and V. I. Klimov, Phys. Rev. Lett. **89**, 186802 (2002).
[9] T. Foerster, Ann. Phys. **2**, 55 (1948).
[10] I. L. Medintz, A. R. Clapp, H. Mattoussi, E. R. Goldman, B. Fisher, and J. M. Mauro, Nat. Mater. **2**, 630 (2003).
[11] M. Achermann, M. A. Petruska, S. Kos, D. L. Smith, D. D. Koleske, and V. I. Klimov, Nature (London) **429**, 642 (2004).
[12] T. Franzl, T. A. Klar, S. Schietinger, A. L. Rogach, and J. Feldmann, Nano Lett. **4**, 1599 (2004).
[13] T. A. Klar, T. Franzl, A. L. Rogach, and J. Feldmann, Adv. Mater. (Weinheim, Ger.) **17**, 769 (2005).
[14] U. Rossow, *Epioptics* (Springer, New York, 1982).
[15] G. Nimtz and B. Schlicht, *Springer Tracts in Modern Physics* (Springer, New York, 1983).
[16] A. Olkhovets, R.-C. Hsu, A. Lipovskii, and F. W. Wise, Phys. Rev. Lett. **81**, 3539 (1998).
[17] J. H. Warner, E. Thomson, A. R. Watt, N. R. Heckenberg, and H. Rubinsztein-Dunlop, Nanotechnology **16**, 175 (2005).
[18] D. Kim, T. Kuwabara, and M. Nakayama, J. Lumin. **119-120**, 214 (2006).
[19] E. Lifshitz, M. Sirota, and H. Porteanu, J. Cryst. Growth **196**, 126 (1999).
[20] M. J. Fernée, E. Thomson, P. Jensen, and H. Rubinsztein-Dunlop, Nanotechnology **17**, 956 (2006).
[21] G. Allan and C. Delerue, Phys. Rev. B **70**, 245321 (2004).
[22] L. Cademartiri, E. Montanari, G. Calestan, A. Migliori, A. Guagliardi, and G. Ozin, J. Am. Chem. Soc. **128**, 10337 (2006).
[23] J. L. Marin, R. Riera, and S. A. Cruz, J. Phys.: Condens. Matter **10**, 1349 (1998).
[24] X. Wang, L. Qu, J. Zhang, X. Peng, and M. Xiao, Nano Lett. **3**, 1103 (2003).
[25] H. Du, C. Chen, R. Krishnan, T. D. Krauss, J. M. Harbold, F. W. Wise, M. G. Thomas, and J. Silcox, Nano Lett. **2**, 1321 (2002).
[26] B. L. Wehrenberg, C. Wang, and P. Guyot-Sionnest, J. Phys. Chem. B **106**, 10634 (2002).
[27] J. J. Peterson and T. D. Krauss, Nano Lett. **6**, 510 (2006).
[28] M. J. Fernée, P. Jensen, and H. Rubinsztein-Dunlop, J. Phys. Chem. C **111**, 4984 (2007).
[29] C. R. Kagan, C. B. Murray, M. Nirmal, and M. G. Bawendi, Phys. Rev. Lett. **76**, 1517 (1996).
[30] T. Franzl, D. S. Kotysh, T. A. Klar, A. L. Rogach, J. Feldmann, and N. Gaponik, Appl. Phys. Lett. **84**, 2904 (2004).
[31] T. Franzl, A. Shavel, A. L. Rogach, N. Gaponik, T. A. Klar, A. Eychmueller, and J. Feldmann, Small **4**, 392 (2005).
[32] O. I. Micic, K. M. Jones, A. Cahill, and A. J. Nozik, J. Phys. Chem. B **102**, 9791 (1998).
[33] S. W. Clark, J. M. Harbold, and F. W. Wise, J. Am. Chem. Soc. **111**, 7302 (2007).
[34] L. Novotny and B. Hecht, *Principles of Nano-Optics* (Cambridge University Press, Cambridge, England, 2006), p. 284.